Physica A 422 (2015) 167–174

Contents lists available at ScienceDirect

Physica A

journal homepage: www.elsevier.com/locate/physa

Generalized relative entropies in the classical limit

A.M. Kowalski [a,b], M.T. Martin [a,c], A. Plastino [a,c,*]

[a] Instituto de Física (IFLP-CCT-Conicet), Fac. de Ciencias Exactas, Universidad Nacional de La Plata, C.C. 727, 1900 La Plata, Argentina
[b] Comision de Investigaciones Científicas (CIC), Argentina
[c] Argentina's National Research Council (CONICET), Argentina

HIGHLIGHTS

- Statistical quantifiers are compared in their ability to describe feature of the route towards the classical limit.
- The normalized Cressie–Read and relative Tsallis ones are shown to be equivalent.
- The Tsallis quantifier is seen to provide a better description than the Kullback–Leibler one.

ARTICLE INFO

Article history:
Received 1 October 2014
Received in revised form 11 December 2014
Available online 23 December 2014

Keywords:
Tsallis relative entropy
Cressie–Read quantifiers
Classical limit
Time-series

ABSTRACT

Our protagonists are (i) the Cressie–Read family of divergences (characterized by the parameter γ), (ii) Tsallis' generalized relative entropies (characterized by the q one), and, as a particular instance of both, (iii) the Kullback–Leibler (KL) relative entropy. In their normalized versions, we ascertain the equivalence between (i) and (ii). Additionally, we employ these three entropic quantifiers in order to provide a statistical investigation of the classical limit of a semiclassical model, whose properties are well known from a purely dynamic viewpoint. This places us in a good position to assess the appropriateness of our statistical quantifiers for describing involved systems. We compare the behaviour of (i), (ii), and (iii) as one proceeds towards the classical limit. We determine optimal ranges for γ and/or q. It is shown the Tsallis-quantifier is better than KL's for $1.5 < q < 2.5$.

1. Introduction

Entropic quantifiers (see as examples Refs. [1–4], and references therein) are useful in the study of time series' underlying dynamics. Systems that are characterized by either long-range interactions, long-term memories, or multi-fractality are best described by a generalized statistical mechanics' formalism [5] usually alluded to as deformed, Tsallis' q-statistics. The basic associated entity is the entropy [$q \in \mathcal{R}$ $(q \neq 1)$]

$$S_q = \frac{1}{(q-1)} \sum_{i=1}^{n} p_i \left[1 - {p_i}^{q-1}\right], \tag{1}$$

p_i being probabilities associated with the n different system-configurations. The entropic index (or deformation parameter) q describes the deviations of Tsallis entropy from the standard Boltzmann–Gibbs–Shannon-one. One has

$$S = -\sum_{i=1}^{n} p_i \ln p_i. \tag{2}$$

* Corresponding author at: Instituto de Física (IFLP-CCT-Conicet), Fac. de Ciencias Exactas, Universidad Nacional de La Plata, C.C. 727, 1900 La Plata, Argentina. Tel.: +54 11 4786 8114; fax: +54 11 4786 8114.
E-mail addresses: kowalski@fisica.unlp.edu.ar (A.M. Kowalski), mtmartin@fisica.unlp.edu.ar (M.T. Martin), plastino@fisica.unlp.edu.ar (A. Plastino).

http://dx.doi.org/10.1016/j.physa.2014.12.017
0378-4371/

Shannon's entropy works best for systems composed of either independent subsystems or interacting via short-range forces, whose subsystems can access all the available phase space [6]. For systems exhibiting long-range correlations, memory, or fractal properties, Tsallis' entropy becomes the most convenient quantifier [6–16].

In another vein, we have the Cressie–Read (CR) family of power divergences, defined through a class of additive convex functions. The CR power divergence measure encompasses a broad family of test statistics that leads to a large family of likelihood functions. They constitute a family of pseudo-distance measures from which to derive empirical probabilities associated with indirect noisy micro and macro data [17].

In order to assess how good these quantifiers are to statistically describe complex scenarios, we will apply the above mentioned quantifiers to a celebrated semiclassical system in its route towards the classical limit [18,19]. The system's dynamics exhibits regular zones, chaotic ones and other regions that, although not chaotic, display complex features. The system has been exhaustively investigated from a purely dynamic viewpoint [19] and also from a statistical one [20–22]. This last kind of study has a pre-requisite: how to extracted information from a time series (TS) [23]. The data at our disposal always possess a stochastic component due to noise [24,25], so that different extraction-procedures attain distinct degrees of quality. We will employ the Bandt and Pompe's approach [26], that determines the probability distribution associated to time series on the basis of the nature of the underlying attractor (see Appendix for the mathematical details).

Summing up, we will use the normalized versions of Tsallis relative entropy [9,27] and Cressie–Read family of divergences [17], to which we add Kullback–Leibler's relative entropy. It will be seen that the normalized CR coincides with the normalized Tsallis relative entropy for a special relationship between q and γ. With these entropies we will compare (i) the probability distribution functions (PDFs) associated to the system's dynamic equation's solutions in their route towards the classical limit [19] with (ii) the PDF associated to the classical solutions.

The relative entropies mentioned above are discussed in Section 2, which briefly recapitulates notions concerning the Tsallis relative entropy, the Kullback–Leibler relative entropy and the CR-divergence family of entropic functionals. As a test-scenario, the semiclassical system and its classical limit are described in Section 3, and the concomitant results are presented in Section 4. Finally, some conclusions are drawn in Section 5.

2. Kullback–Leibler relative entropy, Tsallis relative entropy and Cressie–Read family of divergences

The relative entropies (RE) quantify the difference between two probability distributions P and Q [28]. They provide an estimation of how much information P contains relative to Q and measure the expected number of extra bits required to code samples from P when using a code based on Q, rather than using a code based on P [28]. They can also be regarded as entropic *distances*, alternative means for comparing the distribution Q to P. The best representative is the Kullback–Leibler's (KL) one, based on the Shannon canonical measure (2). For two normalized, discrete probability distribution functions (PDF) $P = (p_1, \ldots, p_n)$ and $Q = (q_1, \ldots, q_n)$ $(n > 1)$, one has

$$D_{\mathrm{KL}}(P, Q) = \sum_{i=1}^{n} p_i \ln\left(\frac{p_i}{q_i}\right), \tag{3}$$

with $D_{\mathrm{KLsn}}(P, Q) \geq 0$. $D_{\mathrm{KL}}(P, Q) = 0$ if and only if $P = Q$. One assumes that either $q_i \neq 0$ for all values of i, or that if one $q_i = 0$, then $p_i = 0$ as well [29]. In such an instance people take $0/0 = 1$ [29] (also, $0 \ln 0 = 0$, of course). It is convenient to work with a normalized KL-version, for the sake of a better comparison between different results. In this way the quantifier's values are restricted to the $[0, 1]$ interval, via division by its maximum allowable value. If we divide D by $\ln n$, expression (3) becomes

$$D^{N}_{\mathrm{KL}}(P, Q) = \frac{1}{\ln n} \sum_{i=1}^{n} p_i \ln\left(\frac{p_i}{q_i}\right), \tag{4}$$

with $0 \leq D^{N}_{\mathrm{KL}} \leq 1$. We will work with Eq. (4). KL can be seen as a particular case of the generalized Tsallis relative entropy [9,27]

$$D_q(P, Q) = \frac{1}{q-1} \sum_{i=1}^{n} p_i \left[\left(\frac{p_i}{q_i}\right)^{q-1} - 1\right], \tag{5}$$

when $q \to 1$ [9,27]. $D_q(P, Q) \geq 0$ if $q \geq 0$. For $q > 0$ one has $D_q(P, Q) = 0$ if and only if $P = Q$. For $q = 0$ one has $D_q(P, Q) = 0$ for all P and Q.

We pass now to define the Cressie–Read (CR) family of divergence measures [17]:

$$I(P, Q, \gamma) = \frac{1}{\gamma(\gamma+1)} \sum_{i=1}^{n} p_i \left[\left(\frac{p_i}{q_i}\right)^{\gamma} - 1\right], \tag{6}$$

where γ is a parameter that indexes members of the CR family. CR differs from $D_q(P, Q)$ because of the condition $I(P, Q, \gamma) \geq 0$, **for all** γ. In the two special cases where $\gamma = 0$ or -1, the notation $I(P, Q, 0)$ and $I(P, Q, -1)$ are to be interpreted as the limits, $\lim_{\gamma \to 0}$ or $\lim_{\gamma \to -1}$, respectively [17]. The $\gamma = 0$ case, corresponds to $D_{\mathrm{KL}}(p, q)$ [17], mimicking what happens with $D_q(P, Q)$ when $q \to 1$. On the other hand, $I(P, Q, -1) = D_{\mathrm{KL}}(Q, P)$ [17].

If one wishes to employ normalized $D_q(P, Q)$ and $I(P, Q, \gamma)$ versions for comparison purposes, we must consider two cases. So as to normalize the expression of $D_q(P, Q)$ given by Eq. (5), (a) if $q \geq 1$, we divide by $(n^{q-1} - 1)/(q - 1)$ in the case of computing $D_q(P, Q)$ for the certainty vs. the equiprobability case and (b) if $0 \leq q < 1$, we divide by $(n^{-q} - 1)/(q - 1)$ in the case of computing it for the equiprobability vs. the certainty. We obtain

$$D_q^N(P, Q) = \frac{1}{n^{q-1} - 1} \sum_{i=1}^{n} p_i \left[\left(\frac{p_i}{q_i} \right)^{q-1} - 1 \right], \quad q \geq 1, \tag{7a}$$

$$D_q^N(P, Q) = \frac{1}{n^{-q} - 1} \sum_{i=1}^{n} p_i \left[\left(\frac{p_i}{q_i} \right)^{q-1} - 1 \right], \quad 0 \leq q < 1. \tag{7b}$$

The relation $0 \leq D_q^N(P, Q) \leq 1$. $D_q^N(P, Q) = 0$ holds if and only if $P = Q$.

To normalize the expression (6), we must consider $\gamma \geq 0$ (or $\gamma < 0$) in our studies and divide by $(n^{\gamma} - 1)/\gamma(\gamma + 1)$ in the case of computing $I(p, q, \gamma)$ for the certainty vs. the equiprobability case (or by $(n^{-(\gamma+1)} - 1)/\gamma(\gamma + 1)$ for the equiprobability vs. the certainty). We get

$$I^N(P, Q, \gamma) = \frac{1}{n^{\gamma} - 1} \sum_{i=1}^{n} p_i \left[\left(\frac{p_i}{q_i} \right)^{\gamma} - 1 \right], \quad \gamma \geq 0, \tag{8a}$$

$$I^N(P, Q, \gamma) = \frac{1}{n^{-(\gamma+1)} - 1} \sum_{i=1}^{n} p_i \left[\left(\frac{p_i}{q_i} \right)^{\gamma} - 1 \right], \quad \gamma < 0. \tag{8b}$$

One has $0 \leq I^N(P, Q, \gamma) \leq 1$. Also, $I^N(P, Q, \gamma) = 0$, if and only if $P = Q$. It is easy to see, and this is our first result, that $I^N(P, Q, \gamma)$ **coincides** with $D_q^N(P, Q)$ by setting $\gamma = q - 1$. In this way, the normalized Tsallis relative entropy can be also *defined or extended to be nonnegative for all q*.

3. Classical–quantum transition

This is a really important issue. The classical limit of quantum mechanics (CLQM) can be viewed as one of the frontiers of physics [30–34], being the origin of exciting discussion (see, for example, Refs. [30,31] and references therein). An interesting sub-issue is that of "quantum" chaotic motion. Recent advances made by distinct researchers are available in Ref. [35] and references therein. Another related interesting sub-issue is that of the generalized uncertainty principle (GUP) [36,37]. Zurek Habib [32–34] and others investigated the emergence of the classical world from Quantum Mechanics.

We are interested here in a semiclassical perspectives, for which several directions can be found exist: the historical WKB and Born–Oppenheimer approaches, etc. The two-interacting systems, considered by Bonilla and Guinea [38], Cooper et al. [18], and Kowalski et al. [19,39], constitute composite models in which one system is classical and the other is quantal. This makes sense when the quantum effects of one of the two systems are negligible in comparison to those of the other one [19]. Examples encompass Bloch equations, two-level systems interacting with an electromagnetic field within a cavity, and collective nuclear motion. We are concerned below with a bipartite system representing the zero-th mode contribution of a strong external field to the production of charged meson pairs [18,19], whose Hamiltonian reads

$$\hat{H} = \frac{1}{2} \left(\frac{\hat{p}^2}{m_q} + \frac{{P_A}^2}{m_{cl}} + m_q \omega^2 \hat{x}^2 \right). \tag{9}$$

$\hat{x}$ and $\hat{p}$ above are quantum operators, while A and P_A are classical canonical conjugate variables. The term $\omega^2 = {\omega_q}^2 + \mathrm{e}^2 A^2$ is an interaction one introducing nonlinearity, with ω_q a frequency. m_q and m_{cl} are masses, corresponding to the quantum and classical systems, respectively. As shown in Ref. [39], when faced with Eq. (9), one has to deal with the autonomous system of nonlinear coupled equations:

$$\begin{aligned}
&\frac{\mathrm{d}\langle \hat{x}^2 \rangle}{\mathrm{d}t} = \frac{\langle \hat{L} \rangle}{m_q}; \qquad \frac{\mathrm{d}\langle \hat{p}^2 \rangle}{\mathrm{d}t} = -m_q \, \omega^2 \langle \hat{L} \rangle \\
&\frac{\mathrm{d}\langle \hat{L} \rangle}{\mathrm{d}t} = 2 \left(\frac{\langle \hat{p}^2 \rangle}{m_q} - m_q \, \omega^2 \langle \hat{x}^2 \rangle \right) \\
&\frac{\mathrm{d}A}{\mathrm{d}t} = \frac{P_A}{m_{cl}} \qquad \frac{\mathrm{d}P_A}{\mathrm{d}t} = -\mathrm{e}^2 m_q \, A \langle \hat{x}^2 \rangle \\
&\hat{L} = \hat{x}\hat{p} + \hat{p}\hat{x},
\end{aligned} \tag{10}$$

derived from Ehrenfest's relations for quantum variables and from canonical Hamilton's equations for classical ones [39]. To investigate the classical limit one needs also to consider the classical counterpart of the Hamiltonian (9), in which all

variables are classical. In such case, Hamilton's equations lead to a classical version of (10). One can consult Ref. [39] for further details. The classical equations are identical in form to Eqs. (10), after replacing quantum mean values by classical variables. The classical limit is obtained considering the limit of a "relative energy" [19]

$$E_r = \frac{|E|}{I^{1/2}\omega_q} \to \infty, \tag{11}$$

where E is the total energy of the system and I is an invariant of the motion described by the system (10). I relates to the Uncertainty Principle:

$$I = \langle \hat{x}^2 \rangle \langle \hat{p}^2 \rangle - \frac{\langle \hat{L} \rangle^2}{4} \geq \frac{\hbar^2}{4}. \tag{12}$$

To tackle this system one appeals to numerical solution. The pertinent analysis is effected by plotting quantities of interest against E_r, that ranges in $[1, \infty]$. For $E_r = 1$ the quantum system acquires all the energy $E = I^{1/2}\omega_q$ and the quantal and classical variables get located at the fixed point ($\langle \hat{x}^2 \rangle = I^{1/2}/m_q\omega_q$, $\langle \hat{p}^2 \rangle = I^{1/2} m_q \omega_q$, $\langle \hat{L} \rangle = 0$, $A = 0$, $P_A = 0$) [39]. Since $A = 0$, the two systems become uncoupled. For $E_r \sim 1$ the system is of an almost quantal nature, with a quasi-periodic dynamics [19].

As E_r augments, quantum features are rapidly lost and a semiclassical region is entered. From a given value ${E_r}^{cl}$, the morphology of the solutions to Eqs. (10) begins to resemble that of classical curves [19]. One indeed achieves convergence of Eqs. (10)'s solutions to the classical ones. For very large E_r-values, the system thus becomes classical. Both types of solutions coincide. We regard as semiclassical the region $1 < E_r < {E_r}^{cl}$. Within such an interval we highlight the important value $E_r = {E_r}^{\mathcal{P}}$, at which chaos emerges [39]. We associate to our physical problem a time-series given by the E_r-evolution of appropriate expectation values of the dynamical variables and use entropic relations so as to compare the PDF associated to the purely classical dynamic solution with the semiclassical ones, as these evolve towards the classical limit.

4. Numerical results

Since we have verified the equivalence between Tsallis' and CR's normalized results, we can content ourselves with depicting only the former ones. We parameterize things then with q and use Eqs. (7). Note that (7b) is valid for all $q < 1$. In our numerical study we have used $m_q = m_{cl} = \omega_q = e = 1$. As for the initial conditions needed to tackle Eqs. (10), we employed $E = 0.6$. Thus, we fixed E and then varied I in order to determine the distinct values of E_r. We employed 55 different values for I. Further, we set $\langle L \rangle(0) = L(0) = 0, A(0) = 0$ (for the quantum and for the classical instances), while $x^2(0)$ and $\langle x^2 \rangle(0)$ take values in the intervals $(0, 2E)$, $(E - \sqrt{E^2 - I}, E + \sqrt{E^2 - I})$, respectively, with $I \leq E^2$. Here, ${E_r}^{\mathcal{P}} = 3.3282$ and ${E_r}^{cl} = 21.55264$. At ${E_r}^{M}$ we encounter a maximum of the quantifier called statistical complexity, and ${E_r}^{M} = 8{,}0904$.

Remember that our "signal" represents the system's state at a given E_r. Sampling this signal we can extract several PDFs using the Band and Pompe technique (see Appendix), for which it is convenient to adopt the largest D-value that verifies the condition $D! \ll M$ (see Appendix). Such value is here $D = 6$, because we will be concerned with vectors whose components comprise at least $M = 5000$ data-points for each orbit. For verification purposes, we also employed $D = 5$, without detecting appreciable changes.

In evaluating our relative entropies, our P-distributions are extracted from the time-series for the different E_r's, while Q is associated to the classical PDF. We consider only the case $q \geq 1$. Figs. 1, 2, and 3 represent the Kullback divergence $D^N_{\mathrm{KL}}(P, Q)$ and the generalized relative entropy $D^N_q(P, Q)$ (i.e., the (pseudo) distance (psd) between PDFs) for different values of q. All curves show that (i) the maximal psd's between the pertinent PDFs are encountered for $E_r = 1$, corresponding to the purely quantal situation and (ii) that they grow smaller as E_r augments, tending to vanish for $E_r \to \infty$. Of course, one finds that the results depend upon q. We highlight in our plots special E_r-values whose great dynamical significance was pointed out above. These are ${E_r}^{\mathcal{P}}$ (chaos begins), ${E_r}^{cl}$ (start of the transitional zone), and ${E_r}^{M}$ [40].

As a general trend, when q grows, the size of the transition region diminishes and that of the classical zone grows. Results are acceptable for the Kullback divergence and for $q = 1.5$, as depicted in Figs. 1, although the size of the transition region looks overestimated if one considers the location of ${E_r}^{cl}$. Things improve for $q = 2$ (Fig. 2). We can assert that our description is optimal for $1.5 < q < 2.5$. The description, instead, lose quality for $q \geq 2.5$. The classical region grows too much. It starts at $E_r < {E_r}^{cl}$ (see Fig. 3(a)). Starting with $q = 5$ (see Fig. 3(b)), the transition region disappears for all practical purposes.

In Fig. 4 we plot the ratio $D^N_q(P, Q)_{E_r=6}/D^N_q(P, Q)_{E_r=1}$, vs. q. The E_r in the denominator is that of the purely quantum case. The one in the numerator corresponds to the middle-transition region. A similar ratio is displayed in Fig. 5, but for a numerator corresponding to $E_r = 10.5247$. In both plots the KL divergence is included ($q = 1$). We observe in our graphs that relative entropies diminish as q grows. This happens more rapidly in the transition than in the quantum zones. The diminution rate grows with E_r.

5. Conclusions

We have shown that the normalized CR divergences $I^N(P, Q, \gamma)$ **coincide** with the Tsallis relative ones, $D^N_q(P, Q)$. The equivalence is given by the relation $\gamma = q - 1$, for $\gamma \geq -1$ (or $q \geq 0$). By means of this relation, the normalized Tsallis relative entropy can be also found to be nonnegative for all q. Thus, it suffices to investigate the behaviour of $D^N_q(P, Q)$.

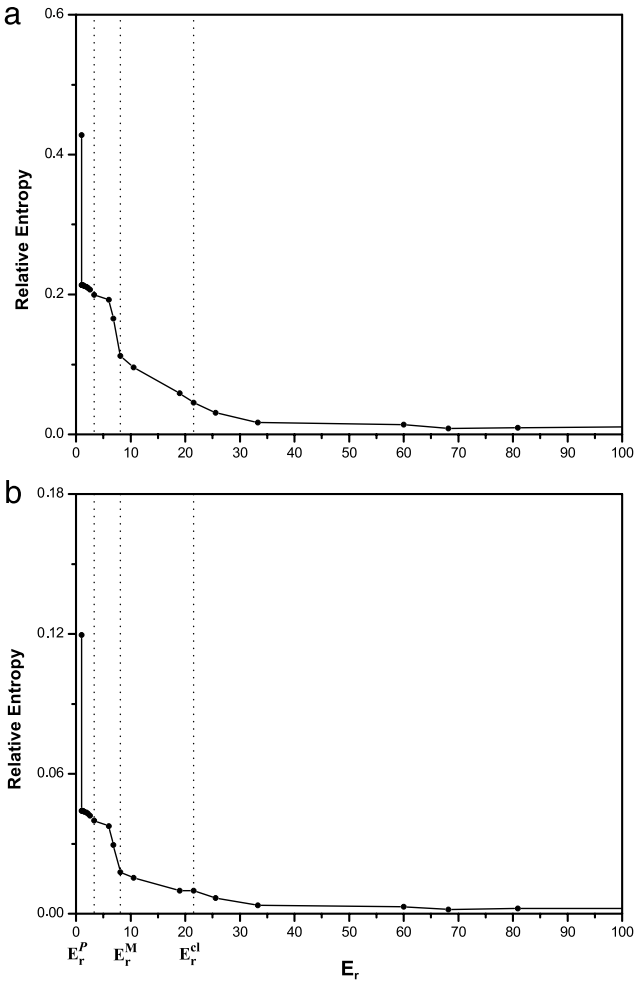

Fig. 1. (a) The normalized Kullback divergence $D_{KL}^N(P, Q)$ is plotted *vs.* E_r. (b) Normalized generalized relative entropy $D_q^N(P, Q)$ *vs.* E_r for $q = 1.5$. We observe that (i) the maximal distance (pseudodistance) between the pertinent PDFs is encountered for $E_r = 1$, corresponding to the purely quantal situation and (ii) that it grows smaller as E_r augments, tending to vanish for $E_r \to \infty$. Results are acceptable for both curves, although the size of the transition region looks overestimated if one considers the location of $E_r{}^{cl}$.

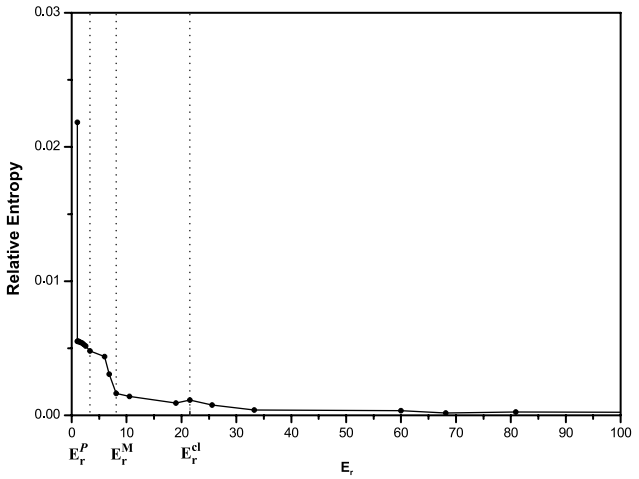

Fig. 2. $D_q^N(P, Q)$ is plotted *vs.* E_r for $q = 2$. As in Figs. 1, the maximal distance (pseudodistance) is encountered for $E_r = 1$. Distance (pseudodistance) grows smaller as E_r augments. The description of the three dynamical regions is optimal.

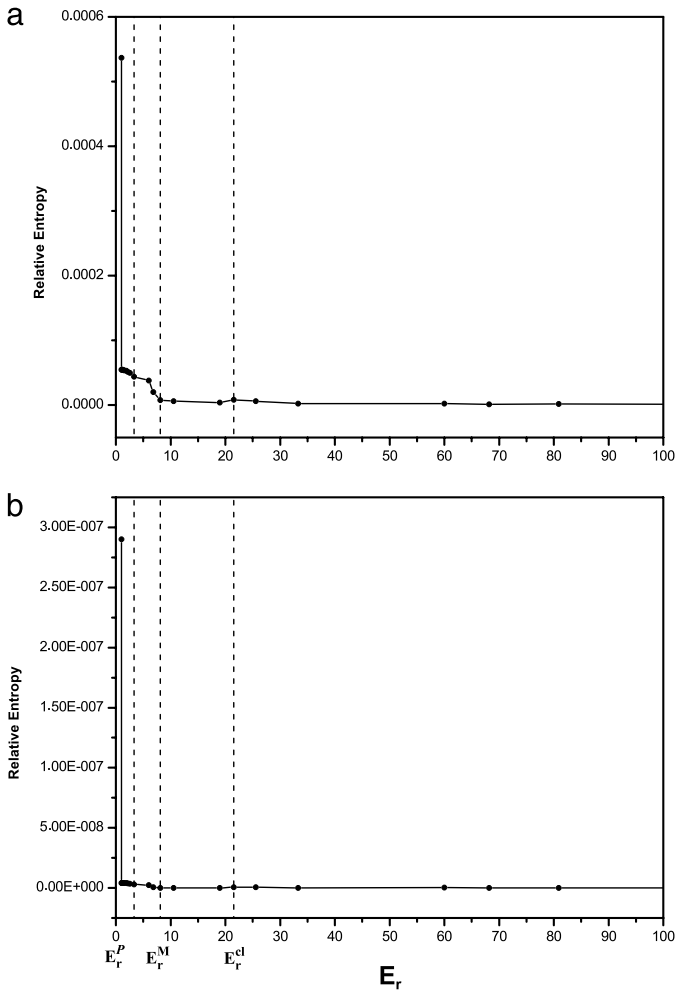

Fig. 3. $D_q^N(P, Q)$ is plotted *vs.* E_r for (a) $q = 3$ and (b) $q = 5$. As in Figs. 1 and 2, the maximal distance (pseudodistance) is encountered for $E_r = 1$ and it grows smaller as E_r augments. The description instead lose quality. In Fig. 3(b), the transition region disappears for all practical purposes.

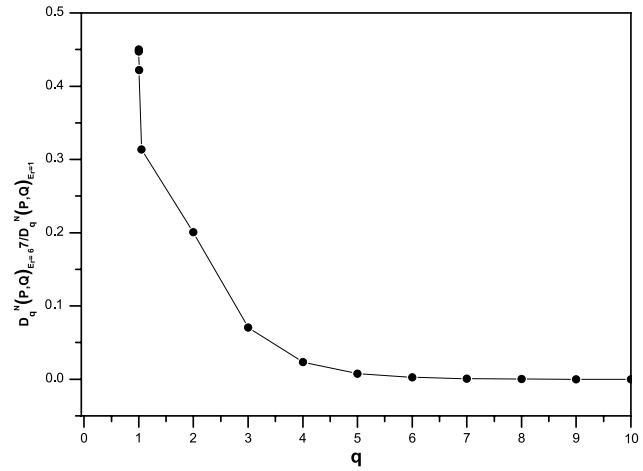

Fig. 4. We plot the ratio between $D_q^N(P, Q)$ (for $E_r = 6$) and that for $E_r = 1$ (both for the same q), i.e., $D_q^N(P, Q)_{E_r=6}/D_q^N(P, Q)_{E_r=1}$, *vs.* q. The KL divergence is the particular instance $q = 1$. Relative entropies diminish as q grows, but this happens more rapidly in the transition than in the quantum zone.

The physics involved is that of a special bipartite semiclassical system that represents the zero-th mode contribution of a strong external field to the production of charged meson pairs [18,19]. The system is endowed with three dynamical regions,

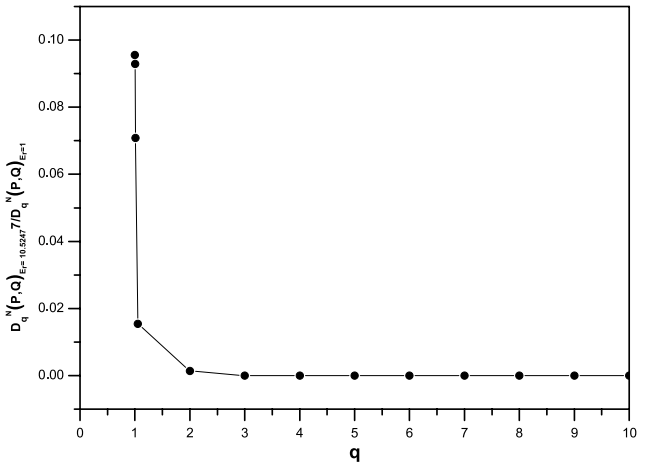

Fig. 5. We plot the ratio between the $D_q^N(P, Q)$ corresponding to $E_r = 10.5247$ and $E_r = 1$, i.e., $D_q^N(P, Q)_{E_r=10.5247}/D_q^N(P, Q)_{E_r=1}$, *vs.* q. (KL is the $q = 1$ case.) As in Fig. 4, we observe that relative entropies diminish more rapidly in the transition than in the quantum zone as q grows. The diminution rate grows with E_r.

as characterized by the values adopted by the parameter E_r. We have a purely quantal zone ($E_r \simeq 1$), a semiclassical one, and finally, a classical sector. The two later ones are separated by the value $E_r{}^{cl}$ (see Section 3). In evaluating relative entropies ((4) and (7)), the P-PDF's are extracted from time series associated to different E_r-values, while Q is always the PDF that describes the classical scenario. We are thus speaking of "distances" between the PDF's extracted in the path towards the classical limit and the classical PDF.

Our first result in this respect is that the maximum distance is attained for the purely quantum case $E_r = 1$, as one would expect. Also, this distance decreases as E_r augments, tending to vanish for $E_r \to \infty$. A second result is that the appropriateness of the statistical description depends upon q, being related to how well the transition zone is represented. For $1 \leq q \leq 1.5$, the size of this zone is overestimated, while for $q \geq 2.5$ it is underestimated. This conclusion arises by consideration, in both cases, of the location of $E_r{}^{cl}$. For $q \geq 2.5$, things seriously deteriorate. In particular, for $q > 5$ the transition region entirely disappears. Our representation becomes thus optimal for $1.5 < q < 2.5$. Accordingly, Tsallis' quantifier in this q-interval is seen to provide a better process' description than the Kullback–Leibler one (identified here as the one for $q = 1$).

Appendix

A.1. PDF based on Bandt and Pompe's methodology

To use the Bandt and Pompe [26] methodology for evaluating the probability distribution P associated with the time series (dynamical system), one starts by considering partitions of the pertinent D-dimensional space that will hopefully "reveal" relevant details of the ordinal structure of a given one-dimensional time series $\mathcal{S}(t) = \{x_t;\ t = 1, \ldots, M\}$, with embedding dimension $D > 1$ and time delay τ.

We will take here $\tau = 1$ as the time delay [26] and be interested in "ordinal patterns", of order D [26,41], generated by

$$(s) \mapsto \left(x_{s-(D-1)}, x_{s-(D-2)}, \ldots, x_{s-1}, x_s\right), \tag{A.1}$$

which assigns to each time the D-dimensional vector of values at times $s, s-1, \ldots, s-(D-1)$. Clearly, the greater the D-value, the more information on the past is incorporated into our vectors. By "ordinal pattern" related to the time (s), we mean the permutation $\pi = (r_0, r_1, \ldots, r_{D-1})$ of $[0, 1, \ldots, D-1]$ defined by

$$x_{s-r_{D-1}} \leq x_{s-r_{D-2}} \leq \cdots \leq x_{s-r_1} \leq x_{s-r_0}. \tag{A.2}$$

In this way the vector defined by Eq. (A.1) is converted into a unique symbol $\hat{x}_i$. Thus, a permutation probability distribution $P_x = \{p(\hat{x}_i), i = 1, \ldots, D!\}$ is obtained from the time series x_i. The probability distribution P is obtained once we fix the embedding dimension D and the time delay τ. The former parameter plays an important role for the evaluation of the appropriate probability distribution, since D determines the number of accessible states, $D!$, and tells us about the necessary length M of the time series needed in order to work with a reliable statistics, i.e. it must be $D! \ll M$. In particular, Bandt and Pompe [26] suggest for practical purposes to work with $3 \leq D \leq 7$. For more details see Ref. [41].

References

[1] C.E. Shannon, Bell Syst. Tech. J. 27 (1948) 379, 623.
[2] J.S. Shiner, M. Davison, P.T. Landsberg, Phys. Rev. E 59 (1999) 1459.

[3] R. López-Ruiz, H.L. Mancini, X. Calbet, Phys. Lett. A 209 (1995) 321.
[4] P.W. Lamberti, M.T. Martin, A. Plastino, O.A. Rosso, Physica A 334 (2004) 119.
[5] C. Tsallis, J. Stat. Phys. 52 (1988) 479.
[6] R. Hanel, S. Thurner, Physica A 380 (2007);
G. Kaniadakis, Phys. Rev. E 66 (2002) 056125;
M.P. Almeida, Physica A 300 (2001) 424;
J. Naudts, Physica A 316 (2002) 323.
[7] P.A. Alemany, D.H. Zanette, Phys. Rev. E 49 (1994) R956.
[8] C. Tsallis, Fractals 3 (1995) 541.
[9] C. Tsallis, Phys. Rev. E 58 (1998) 1442.
[10] S. Tong, A. Bezerianos, J. Paul, Y. Zhu, N. Thakor, Physica A 305 (2002) 619.
[11] C. Tsallis, C. Anteneodo, L. Borland, R. Osorio, Physica A 324 (2003) 89.
[12] O.A. Rosso, M.T. Martín, A. Plastino, Physica A 320 (2003) 497.
[13] L. Borland, Europhys. News 36 (2005) 228.
[14] H. Huang, H. Xie, Z. Wang, Phys. Lett. A 336 (2005) 180.
[15] D.G. Pérez, L. Zunino, M.T. Martín, M. Garavaglia, A. Plastino, O.A. Rosso, Phys. Lett. A 364 (2007) 259.
[16] M. Kalimeri, C. Papadimitriou, G. Balasis, K. Eftaxias, Physica A 387 (2008) 1161.
[17] N. Cressie, T. Read, J. R. Stat. Soc. Ser. B 46 (1984) 440;
Goodness of Fit Statistics for Discrete Multivariate Data, Springer, New York, 1988.
[18] F. Cooper, J. Dawson, S. Habib, R.D. Ryne, Phys. Rev. E 57 (1998) 1489.
[19] A.M. Kowalski, A. Plastino, A.N. Proto, Phys. Lett. A 297 (2002) 162.
[20] A.M. Kowalski, M.T. Martín, A. Plastino, O.A. Rosso, Physica D 233 (2007) 21.
[21] A.M. Kowalski, M.T. Martín, A. Plastino, L. Zunino, Physica A 388 (2009) 1985.
[22] A.M. Kowalski, A. Plastino, Physica A 388 (2009) 4061.
[23] A.M. Kowalski, M.T. Martín, A. Plastino, G. Judge, Entropy 14 (2012) 1829.
[24] H. Wold, A Study in the Analysis of Stationary Time Series, Almqvist and Wiksell, Upsala, Sweden, 1938.
[25] J. Kurths, H. Herzel, Probability theory and related fields, Physica D 25 (1987) 165.
[26] C. Bandt, B. Pompe, Phys. Rev. Lett. 88 (2002) 174102:1.
[27] L. Borland, A.R. Plastino, C. Tsallis, J. Math. Phys. 39 (1998) 6490. and its Erratum, 1999, 40, 2196.
[28] A.M. Kowalski, R.D. Rossignoli, E.M.F. Curado (Eds.), Concepts and Recent Advances in Generalized Information Measures and Statistics, Bentham Science Publishers, 2013.
[29] http://en.wikipedia.org/wiki/Kullback–Leiblerdivergence.
[30] J.J. Halliwell, J.M. Yearsley, Phys. Rev. A 79 (2009) 062101:1.
[31] M.J. Everitt, W.J. Munro, T.P. Spiller, Phys. Rev. A 79 (2009) 032328:1.
[32] H.D. Zeh, Found. Phys. Lett. 12 (1999) 197.
[33] W.H. Zurek, Phys. Rev. D 24 (1981) 1516.
[34] W.H. Zurek, Rev. Modern Phys. 75 (2003) 715.
[35] A.M. Kowalski, M.T. Martín, A. Plastino, A.N. Proto, Internat. J. Bifur. Chaos 13 (2003) 2315.
[36] A. Tawfik, J. Cosmol. Astropart. Phys. 1307 (2003) 040.
[37] E. El Dahab, A. Tawfik, e-Print: 2014. arXiv:1401.3164 [gr-qc].
[38] L.L. Bonilla, F. Guinea, Phys. Rev. A 45 (1992) 7718.
[39] A.M. Kowalski, M.T. Martín, J. Nuñez, A. Plastino, A.N. Proto, Phys. Rev. A 58 (1998) 2596.
[40] A.M. Kowalski, A. Plastino, Physica A 391 (2012) 5375.
[41] M. Zanin, L. Zunino, O.A. Rosso, D. Papo, Entropy 14 (2012) 1553.